Supporting Information

Bachovchin et al. 10.1073/pnas.1015248108

SI Materials and Methods

Materials. FP-biotin (1, 2) and FP-rhodamine (3) were synthesized following previously described protocols. Demethylated-specific PP2A (clone 4b7), methylated-specific PP2A (clone 2A10), total PP2A, and PME-1 antibodies were purchased from Millipore. Anti α-tubulin antibodies were purchased from NeoMarkers.

Recombinant PME-1 Protein Expression and Purification. Human wild-type *PME-1* was subcloned into the expression vector pET-45b(+) (Novagen). BL21 (DE3) *Escherichia coli* containing this vector was grown in LB media containing 75 mg/L carbenicillin with shaking at 37 °C to an OD_{600} of 0.5. The cells were then induced with 1 mM IPTG and harvested 4 h later by centrifugation. Cells were lysed by stirring for 20 mins at 4 °C in 50 mM Tris-HCl (pH 8.0) with 150 mM NaCl and supplemented with 1 mg/mL lysozyme and 1 mg/mL DNase I. The lysate was then sonicated and centrifuged at 10,000 × *g* for 10 min. Talon cobalt affinity resin (Clontech; 400 μL of slurry/g of cell paste) was added to the supernatant, and the mixture was rotated at room temperature for 1 h. Beads were collected by centrifugation at 700 × *g* for 3 min, washed twice with Tris buffer, and applied to a 1 cm column. The column was washed twice with Tris buffer (10 mL/400 μL of resin slurry) and Tris buffer with 500 mM NaCl once. The bound protein was eluted by the addition of 100 mM imidazole (2 mL/400 μL of resin). Imidazole was removed by passage over a Sephadex G-25M column (GE Healthcare). Protein concentration was determined using the BioRad DC Protein Assay kit. These conditions yielded pure (>95% by SDS/PAGE) PME-1 at approximately 5 mg/L of culture. A S156A mutation was introduced into the pET-45b(+) construct using the Quikchange Site-Directed Mutagenesis Kit (Stratagene), and the resulting mutant protein was expressed identically and isolated with a similar yield.

PME-1 Fluopol-ABPP Assay. Prior to the start of the assay, 4.0 μL of Assay Buffer [0.01% Pluronic F-127 (Invitrogen), 50 mM Tris-HCl pH 8.0, 150 mM NaCl, 1 mM DTT (Invitrogen)] containing 1.25 μM of PME-1 protein was dispensed into 1536 microtiter plates. Next, 30 nL of test compound in DMSO or DMSO alone (0.59% final concentration DMSO; 5.9 μM compound) was added to the appropriate wells and incubated for 30 minutes at 25 °C. The assay was started by dispensing 1.0 μL of 375 nM FP-Rh probe in assay buffer to all wells. Plates were centrifuged and after 45 min of incubation at 25 °C, fluorescence polarization was read on a Viewlux microplate reader (PerkinElmer) using a BODIPY TMR FP filter set and a BODIPY dichroic mirror (excitation = 525 nm, emission = 598 nm). Fluorescence polarization was read for 15 seconds for each polarization plane (parallel and perpendicular). The well fluorescence polarization value (mP) was obtained via the PerkinElmer Viewlux software. The percent inhibition for each compound was calculated as follows: Percent inhibition = $(\text{Test}_{\text{Compound}}\text{mP-median}_{\text{Negative}}\text{Control}_{\text{mP}})/(\text{median}_{\text{Positive Control}}\text{mP-median}_{\text{Negative}}\text{Control}_{\text{mP}}) * 100$. The test compound was as defined as wells containing PME-1 in the presence of test compound, negative controls were defined as wells containing PME-1 and DMSO, and positive controls were defined as wells containing no PME-1 protein. A mathematical algorithm was used to determine nominally inhibiting compounds in the primary screen. Two values were calculated: (*i*) the average percent inhibition of all compounds tested, and (*ii*) three times their standard deviation. The sum of these two values was used as a cutoff parameter; i.e.. any compound that exhibited greater inhibition than the cutoff parameter (26.13%) was declared active. The reported PubChem Activity Score (http://pubchem.ncbi.nlm.nih.gov/) has been normalized to 100% observed primary inhibition. Negative % inhibition values are reported as activity score zero. The activity score range for active compounds is 100-7, for inactive 7-0.

Cell Culture and Preparation of Human Cell Line Proteomes. MDA-MB-231 cells were grown in L15 media supplemented with 10% fetal bovine serum at 37 °C in a CO_2 free incubator. HEK 293T cells were grown in DMEM with 10% fetal bovine serum at 37 °C with 5% CO_2. For in vitro experiments, cells were grown to 100% confluency, washed two times with PBS, and scraped. Cell pellets were isolated by centrifugation at 1,400 × *g* for 3 min. The pellets were resuspended in 500 μL PBS (pH 7.5), sonicated, and centrifuged (64,000 × *g*, 45 min) to provide the soluble fraction as the supernatant and the membrane fraction as the pellet. For in situ experiments, compounds were directly added to the cell culture media for the indicated time before the cells were washed and scraped. The cell pellets were isolated by centrifugation at 1,400 × *g* for 3 min, resuspended in 500 μL PBS (pH 7.5), and sonicated. 250 μL of this total cell extract was saved for PP2A methylation analysis by Western blotting (described below), and the remainder was separated into membrane and soluble fractions as described above. To overexpress PME-1 or GFP in HEK 293T cells, the genes encoding PME-1 and GFP were cloned into a modified version of pCLNCX vector (Imgenex) and stable cell lines were generated as described previously (4). Total protein concentration of each fraction was determined using a protein assay kit (BioRad). Samples were stored at −80 °C until use.

Competitive ABPP Assays in Proteomes. For in vitro experiments, proteomes were diluted to 1 mg/mL in PBS (pH 7.5) and incubated with DMSO or compound for 30 min at 25 °C (25 μL total reaction volume). FP-rhodamine was then added at a final concentration of 2 μM. After 45 min, the reactions were quenched with 2× SDS/PAGE loading buffer (reducing), separated by SDS/PAGE (10% acrylamide), and visualized in-gel with a Hitachi FMBio IIe flatbed fluorescence scanner (MiraiBio). For in situ experiments, proteomes were diluted to 1 mg/mL in PBS and directly labeled with FP-rhodamine (2 μM) for 45 min and analyzed as described above.

Determination of IC_{50} Values. For determination of in vitro IC_{50} values, compounds were incubated in MDA-MB-231 soluble proteomes (1 mg/mL, 25 μL total volume) at the indicated concentrations (performed in triplicate) for 45 min at 37 °C. The samples were then labeled with FP-rhodamine (2 μM) for 45 min, quenched, separated by SDS/PAGE, and visualized by in-gel fluorescence scanning. For determination of in situ IC_{50} values, the soluble fractions from cells treated with compound (1 h, performed in triplicate) were diluted to 1 mg/mL in PBS (25 μL total volume), then labeled with FP-rhodamine (2 μM) for 45 min, and analyzed as described above. The percentage activity remaining was determined by measuring the integrated optical intensity of the bands using ImageJ software. IC_{50} values were determined from a dose-response curve generated using Prism software (GraphPad).

Assessing the Reversibility of ABL127 Inhibition. Purified wild-type PME-1 (500 nM, 2.6 mL total volume in PBS) was incubated with DMSO or ABL127 (5 μM) at 25 °C. After 30 min, 100 μL was removed from each reaction (Fraction A). The remaining 2.5 mL of each reaction was passaged over a Sephadex G-25M column (GE Healthcare) and eluted in a volume of 3.5 mL PBS (Fraction B). 100 μL of both fractions A and B were labeled with FP-rhodamine (2 μM). After 30 min, the reactions were quenched with 2× SDS/PAGE loading buffer, separated by SDS/PAGE, and analyzed by in-gel fluorescence scanning. Gels were then subjected to Coomassie staining with Instantblue (Expedeon) to verify equivalent protein loading.

Detection of Modified and Unmodified Tryptic Peptides from ABL127-Treated Preparations of PME-1. Purified, recombinant PME-1 (10 μM, 25 μl total volume) was incubated with DMSO or ABL127 (50 μM) for 30 min at 25 °C. Urea (50 mg) was added to each reaction and the reactions were diluted with PBS (75 μL). Each sample was then subsequently incubated with tris-(2-carboxyethyl)phosphine (TCEP, 5 μL of 100 mM stock) and iodoacetamide (10 μL of 100 mM stock) for 30 min each at 25 °C. The samples were diluted with ammonium bicarbonate (25 mM, 375 μL) and subjected to trypsin digestion (Promega; 4 μL of 0.5 μg/μL) overnight at 37 °C in the presence of 2 mM $CaCl_2$. The next day, samples were concentrated, resuspended in ammonium bicarbonate (25 mM, 100 μL) with 0.1% formic acid, and a 10 μl aliquot was pressure-loaded onto a 100 μm (inner diameter) fused silica capillary column with a 5 μm tip that contained 10 cm C18 resin (aqua 5 μm, Phenomenex). LC-MS/MS analysis was performed on an LTQ-Orbitrap mass spectrometer (Discovery, ThermoScientific) coupled to an Agilent 1100 series HPLC. Peptides were eluted from the column using a 125 min gradient of 5%–100% Buffer B (Buffer B: 20% water, 80% acetonitrile, 0.1% formic acid). The flow rate through the column was 0.25 μl/min and the spray voltage was 2.5 kV. The LTQ was operated in data-dependent scanning mode, with one full MS scan (400–1,600 m/z) followed by seven MS/MS scans of the *n*th most abundant ions with dynamic exclusion enabled.

For the results shown in Fig. 3, extracted ion chromatograms (EIC) of the unmodified (top) and ABL127-modified (bottom) PME-1 peptide containing the active-site serine 156 (blue) were generated. The mass window for each EIC, the detected high-resolution mass for each peak, and the charge state for each tryptic peptide are indicated in the figure. In the DMSO-treated sample, we observed a large peak with $m/z = 1382.69$, corresponding to the 5+ charge state of the unmodified PME-1 active-site tryptic peptide (top panel, black). In samples treated with ABL127, however, this peak was absent. Instead, we identified a peak with $m/z = 1449.13$, corresponding to the 5+ charge state of the ABL127-acylated form of the peptide (bottom panel, red). As expected, this peak was not present in the DMSO-treated sample. We found no evidence of carbamoylation of the active-site serine that could potentially result from nucleophilic attack on either one of ABL127's two carbamate groups and would be distinguishable from β-lactam acylation due to a loss of methanol.

Isotopic Competitive ABPP-MudPIT in Human Cell Lines. Cell culture was performed as described above except MDA-MB-231 cells were grown in RPMI-1640 SILAC media (ThermoScientific) and HEK 293T cells were grown in DMEM SILAC media (ThermoScientific) supplemented with dialyzed fetal bovine serum (Gemini) and $^{12}C^{14}N$-lysine and -arginine (Sigma) ("light" cells) or $^{13}C_6{}^{15}N_2$-lysine and -arginine (Isotec) ("heavy" cells). Cells were treated as indicated with DMSO or compound (1 h), and soluble and membrane proteomes were isolated as described above. Light and heavy proteome fractions (0.5 mg each) were combined (1 mL total volume) and were labeled with 5 μM of FP-biotin for 1 hr at 25 °C. After incubation, the membrane proteomes were solubilized with 1% Triton-X and rotated at 4 °C for 1 hr. Enrichment of FP-labeled proteins was achieved as previously described (5, 6). The streptavidin-enriched proteome was washed two times for 3 min with (1) 1% SDS in PBS, (2) 6 M urea in PBS, (3) PBS (pH 7.5), and finally resuspended in 200 μL 8 M urea in 25 mM ammonium bicarbonate. Samples were then prepared for on-bead digestion by reduction with 10 mM TCEP (Sigma) for 30 min at 25 °C and alkylation with 12 mM iodoacetamide (Sigma) for 30 min at 25 °C in the dark. Samples were diluted to 2 M urea with PBS (pH 7.5) and digestions were performed for 12 hr at 37 °C with trypsin (Promega; 4 μL of 0.5 μg/μL) in the presence of 2 mM $CaCl_2$. Lastly, peptide samples were acidified to a final concentration of 5% formic acid.

Digested peptide mixtures were pressure-loaded on a fused silica loading column (250 micron i.d., 360 micron o.d.) packed with 4 cm of reversed-phase resin (Aqua C18, 5micron, 125A, Phenomenex) fitted with the fritted filter (Upchurch). The loading column was attached in-line to a biphasic MudPIT capillary column [100micron i.d., 360micron o.d., packed with 10 cm Aqua C18 reversed-phase resin followed by 3 cm strong cation exchange resin (Partisphere, 5micron, 120A, Whatman) with an in-house pulled tip]. The sample was analyzed by two-dimensional liquid chromatography (2D-LC) separation in combination with tandem mass spectrometry as previously described (6, 7) using an Agilent 1100-series quaternary pump (manual flow-split system) and LTQ-Orbitrap (Discovery for HEK 293T sample analysis or Velos for MDA-MB-231 sample analysis) mass spectrometer using Xcalibur Software (ThermoScientific) outfitted with an in-house fabricated nano-spray platform. Peptides were eluted in a five-step MudPIT experiment (using 0%, 10%, 25%, 80%, and 100% salt bumps of 500 mM aqueous ammonium acetate, each step followed by an increasing gradient of aqueous acetonitrile/0.1% formic acid) and data were collected in data-dependent acquisition mode with dynamic exclusion enabled (repeat count of 1, exclusion duration of 60 s for Discovery or 20 s for Velos). One full MS1 scan (400–1800 m/z) was followed by a series of data-dependent MS2 scans (seven for Discovery, 30 for Velos) of the most abundant ions with monoisotopic precursor selection enabled. All other parameters were left at default values. The MS2 spectra data were extracted from the raw file using RAW Xtractor (version 1.9.7; publicly available at http://fields.scripps.edu/?q=content/download). MS2 spectra data were searched using the SEQUEST algorithm (Version 3.0) (8) against the latest version of the human IPI database concatenated with the reversed database for assessment of false-discovery rate (9). SEQUEST searches allowed for variable oxidation of methionine (+16), static modification of cysteine residues (+57 due to alkylation), and no enzyme specificity. Each dataset was independently searched with light and heavy params files. For the light search, all other amino acids were left at default masses; for the heavy search, static modifications on lysine (8.0142) and arginine (10.0082) were specified. The resulting MS2 spectra matches were assembled into protein identifications and filtered using DTASelect (version 2.0.41) (10) with the –trypstat option, which applies different statistical models for the analysis of tryptic, half-tryptic, nontryptic peptides, and peptides were restricted to fully tryptic using the -y 2 option. DTASelect 2.0 uses a quadratic discriminant analysis to achieve a user-defined maximum peptide false positive rate; the default parameters (maximum false positive rate of 5%) was used for the search; however, the actual false positive rate was much lower (<1%). SILAC ratios were quantified using in-house software (11). The total proteomic data was filtered manually for serine hydrolases containing at least two quantifiable peptides, and data was globally normalized to a control sample where both heavy and light cells were treated with DMSO and mixed in a 1:1 ratio to adjust heavy to light peptide abundance to exactly a 1:1 ratio (correction factor =

1.3light/heavy). In the HEK 293T cell lines, two serine hydrolases, BCHE and CES3, displayed ratios >3light : 1heavy in the control sample that were maintained in the inhibitor-treated sample, and, for simplicity, were excluded from analysis.

Chemistry Space Analysis of the MLPCN Library. Chemistry space coordinates for the chemical structures of and 315,002 MLSMR substances that were screened against PME1 were generated using the software package Diverse Solutions 6.3.2. (Tripos Inc.) following the described methodology (12). 16,000 compounds from the Maybridge compound collection that were screened as a preliminary test of the PME-1 fluopol-ABPP assay were also included in this analysis. Standard hydrogen-suppressed binary BCUTS descriptors were generated from the 2D structures followed by optimization of the chemistry space allowing a maximum of 16 dimensions as described. A 5D chemistry space was obtained:

```
 0.280418    0.509676 NLScaling[0.395317,0.117725] of
   bcut_gastchrg_burden_000.100_R_H.bdf:BCUT, diag =
   Gast.-Huckel charges, off-diag = 10 * Burden's nums *
                0.100, remove Hs, high eig
-0.547135   -0.366027 NLScaling[-0.456299,0.0908346] of
   bcut_gastchrg_burden_000.100_R_L.bdf:BCUT, diag =
   Gast.-Huckel charges, off-diag = 10 * Burden's nums *
                0.100, remove Hs, low eig
 7.64428     10.0443 NLScaling[8.94606,1.30650] of
bcut_haccept_burden_002.500_R_H.bdf:BCUT, diag = h-bond
  acceptor, off-diag = 10 * Burden's nums * 2.500, remove
                        Hs, high eig
 1.72605     2.56110 NLScaling[2.14481,0.423132] of
bcut_hdon or_burden_000.600_R_H.bdf:BCUT, diag = h-bond
  donor, off-diag = 10 * Burden's nums * 0.600, remove Hs,
                        high eig
 2.73170     3.58307 NLScaling[3.16957,0.442155] of
 bcut_tabpolar_burden_000.500_R_H.bdf:BCUT, diag = tab
  polar (A3), off-diag = 10 * Burden's nums * 0.500, remove
                        Hs, high eig
```

Chemistry space coordinates and cell indices using 10 bins per coordinate were then generated (10^5 cells). 12 Maybridge and 746 MLSMR compounds fall outside the space. 12,660 cells are occupied ranging between 1 and 3335 compounds. Figure 2*B* shows all compounds in the first two chemistry space coordinates (the remaining three dimensions are projected into the area shown). The 26 ABLS are shown as (enlarged) squares, other compounds are shown as small circles (dots). Cell occupancy is mapped onto the space and shown by the color of the compounds with red indicating high occupancy and blue the lowest occupancy, illustrating the relatively lower density of the space occupied by the ABLs. The zoomed subspace occupied by the ABLs is shown separately. As expected the most active compounds ABL127 and ABL103 are very close neighbors in this space.

Evaluation of Serine Hydrolases Targeted by ABL127 in Vivo. C57BL/6 mice were treated intraperitoneally with vehicle (18 : 1 : 1 Saline: Emulphor:DMSO) or ABL127 (50 mg kg^{-1}). After 2 hours, the animals were sacrificed and the soluble and membrane fractions of brains were isolated following previously described methods (5). Briefly, mouse brains were Dounce-homogenized in PBS (pH 7.5) followed by a low-speed spin (1,400 × *g*, 5 min) to remove debris. The supernatant was then subjected to centrifugation (64,000 × *g*, 45 min) to provide the soluble fraction as the supernatant and the membrane fraction as the pellet. The soluble proteomes (1 mg/mL) were treated with DMSO or ABL127 (2 μM) for 30 min before incubation with FP-rhodamine (2 μM) for 45 min at 25 °C (25 μL total reaction volume). Reactions were quenched with one volume of standard 2x SDS/PAGE loading buffer (reducing), separated by SDS/PAGE (10% acrylamide), and visualized by in-gel fluorescence scanning.

In addition, both the membrane and soluble proteomes of these brains (1 mg/mL in PBS; 1 mL total volume) were prepared for analysis by ABPP-MudPIT using the FP-Biotin probe as described above. Peptides were eluted in a 5-step MudPIT experiment (using 0%, 10%, 25%, 80%, and 100% salt bumps of 500 mM aqueous ammonium acetate) and data were collected in data-dependent acquisition mode with dynamic exclusion turned on (60 s, repeat of 1) on a Thermo Scientific LTQ ion trap mass spectrometer. Specifically, one full MS (MS1) scan (400–1800 m/z) was followed by 7 MS2 scans of the most abundant ions. The MS2 spectra data were extracted from the raw file using RAW Xtractor (version 1.9.7; publicly available at http://fields.scripps.edu/?q=content/download). MS2 spectra data were searched using the SEQUEST algorithm (Version 3.0) (8) against the latest version of the mouse IPI database concatenated with the reversed database for assessment of false-discovery rates (9). SEQUEST searches allowed for variable oxidation of methionine (+16), static modification of cysteine residues (+57 due to alkylation), and no enzyme specificity. The resulting MS2 spectra matches were assembled into protein identifications and filtered using DTASelect (version 2.0.41) (10) using the –trypstat option. The total proteomic data was filtered for serine hydrolases manually. Serine hydrolases that displayed an average of ≥10 spectral counts from three independent runs are shown.

Immunoblot Analysis. The whole proteomes of cell lines or mouse brains (treated as indicated) were diluted to 2 mg/ml in PBS, denatured with standard 2x SDS/PAGE loading buffer (reducing), separated by SDS/PAGE (10% acrylamide), and analyzed by western blotting using standard methods. Blots were probed using indicated antibodies following manufacturers' instructions, and were visualized and quantified using the Odyssey Imaging System (Li-Cor).

Cycloaddition Reactions with the Clickable Probe ABL112. Click chemistry was performed following previously described protocols (13). For in vitro experiments, soluble proteomes (0.5 mg/mL in PBS) were incubated with DMSO, ABL127, or ent-ABL127 at 25 °C for 30 minutes prior to incubation with ABL112 for 30 min. For in situ experiments, MDA-MB-231 cells were incubated with DMSO or ABL127 for 30 min prior to addition of ABL112 for 2 h. The soluble proteomes from these cells were isolated as described above and diluted to 0.5 mg/mL in PBS. Alkyne-labeled proteomes were then incubated rhodamine-azide (50 μM), followed by TCEP (1 mM), ligand (100 μM), and $CuSO_4$ (1 mM). After 1 h at 25 °C, reactions were analyzed by SDS-PAGE and in-gel fluorescence scanning.

ABL Synthetic Methods

General Information. Analytical data and procedures for the ABLs in the initial screening are reported in our previous work (14). Nucleophilic catalyst PPY* was prepared by literature methods (15). Hydrazine hydrate (Aldrich), propargyl chloroformate (Aldrich), pyridine (Alfa Aesar), K_2CO_3 (Alfa Aesar), absolute ethanol (Pharmco-Aaper), and anhydrous CH_2Cl_2(Aldrich) were purchased and used as received. *N*-Bromosuccinimide was purchased from Alfa Aesar and recrystallized from H_2O prior to use. Cyclopentyl phenyl ketene was prepared according to our previously reported ketene synthesis method (16) from commercially available α-cyclopentylphenylacetic acid (MP Biomedicals) and spectral data matched those previously reported (17). Dimethylazodicarboxylate was purchased from Wako or prepared by literature methods (18).

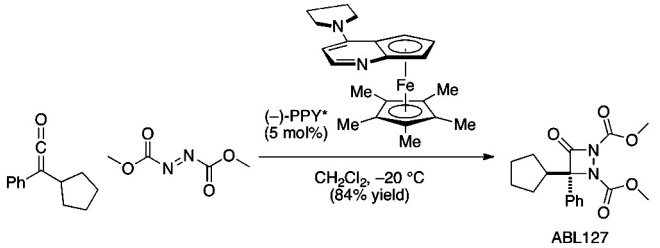

.

Dimethyl 3-cyclopentyl-4-oxo-3-phenyl-1,2-diazetidine-1,2-dicarboxylate (ABL127). (14): In a nitrogen-atmosphere glovebox, a solution of cyclopentyl phenyl ketene (921.4 mg, 4.95 mmol, 1.0 equiv) in CH_2Cl_2 (350 mL) was prepared in a 500 mL round bottom flask. A solution of dimethylazodicarboxylate (722.8 mg, 4.95 mmol, 1.0 equiv) in CH_2Cl_2 (8 mL) was added and the flask was sealed with a rubber septum. In a separate vial, a solution of (−)-PPY* (93.1 mg, 0.25 mmol, 0.05 equiv) in CH_2Cl_2 (4 mL) was prepared and the vial was closed with a septum cap. The flask and vial were removed from the glovebox and the flask containing the golden yellow ketene/azodicarboxylate solution was cooled to −20 °C in an immersion bath. The dark purple catalyst solution was added via syringe leading to an immediate color change to deep blue. The mixture was stirred at −20 °C overnight, and then warmed to ambient temperature and concentrated under vaccum. Flash column chromatography on SiO_2 using 20% EtOAc in hexanes as eluent ($R_f \sim 0.2$) provided ABL127 as a colorless oil (1.3325 g, 84% yield). Spectral data matched those previously reported (14). HPLC analysis found 86% ee (4.6 × 250 mm Chiralpak AD-H column, 10% *i*-PrOH in hexanes eluent, isocratic 1.0 mL/min flow rate, retention times: 18.4 min (minor), 26.6 min (major)).

Separation of enantiomers was achieved by semipreparative HPLC (10 × 250 mm Chiracel OD-H column, 1% *i*-PrOH in hexanes eluent, isocratic 2.75 mL/ min flow rate) provided samples of both ABL127 (major component, retention time: 29.5 min) and ent-ABL127 (minor component, retention time: 27.2 min) with >99% ee

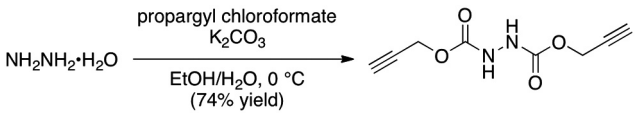

.

Propargyl Hydrazidodicarboxylate (19). To a stirred 0 °C solution of hydrazine hydrate (250.3 mg, 5.0 mmol, 1.0 equiv) in absolute ethanol (3 mL) was added neat propargyl chloroformate (975.5 μL, 10.0 mmol, 2.0 equiv) dropwise. White precipitate formed immediately. When one quarter of the chloroformate had been added, addition of a solution of K_2CO_3 (1.38 g, 10.0 mmol, 2.0 equiv) in deionized water (3 mL) was commenced. The two liquids were added dropwise simultaneously at such a rate that the chloroformate addition was complete just before the addition of the base solution was completed. The resulting heterogeneous mixture was stirred for 1.5 h, during which time it warmed to ambient temperature. The white solid was separated by vacuum filtration through a sintered glass frit and dried on the frit for 45 min. The solid was collected in a vial and further dried under vacuum overnight to provide the hydrazide as a free-flowing white powder (727.9 mg, 74% yield).

^{1}H NMR (500 MHz, CD_3OD) δ 4.72 (d, J = 2.3 Hz, 4H), 2.92 (t, J = 2.3 Hz, 2H);

^{13}C NMR (125 MHz, CD_3OD) δ 158.1, 78.8, 76.4, 53.9;

IR (neat film, NaCl) 3284, 2409, 1704, 1692, 1415, 1341, 1271, 1117, 775, 694, 658 cm^{-1}

LRMS (ES+) m/z: cacld for $C_8H_9N_2O_4[M+H]^+$: 197.1, found 197.0

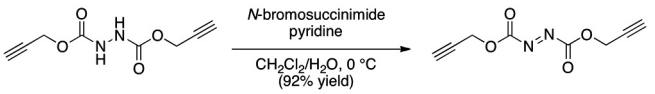

.

Dipropargyl Azodicarboxylate (18). Propargyl hydrazidodicarboxylate (150.0 mg, 0.76 mmol, 1.0 equiv) was suspended in a mixture of CH_2Cl_2 (4 mL) and deionized water (3 mL). Pyridine (56.9 μL, 0.70 mmol, 0.92 equiv) was added to the suspension in one portion and then the mixture was cooled to 0 °C. Solid *N*-bromosuccinimide (136.1 mg, 0.76 mmol, 1.0 equiv) was added in one portion leading to an immediate color change of the organic phase to yellow-orange. The mixture was stirred for 30 min at 0 °C during which time all the solid materials dissolved. The clear colorless aqueous phase was removed and the remaining yellow-orange colored organic phase was washed with water (4 × 2 mL). The organics were dried over $MgSO_4$, filterered, and concentrated under vacuum. The residue was dissolved in toluene (3 mL) and then concentrated again under vacuum to afford an orange oil (136.5 mg, 92% yield) that was used without further purification.

^{1}H NMR (500 MHz, $CDCl_3$) δ 5.02 (app dd, J = 2.4, 1.3 Hz, 4H), 2.65 (app dt, J = 2.4, 1.3 Hz, 2H);

^{13}C NMR (125 MHz, $CDCl_3$) δ 159.4, 77.6, 75.3, 56.5;

IR (neat film, NaCl) 2134, 1788, 1441, 1371, 1267, 1214, 1027, 990, 944, 879, 859, 805, 694, 646, 539 cm^{-1};

LRMS (ES+) m/z: cacld for $C_8H_6N_2O_4Na[M+Na]^+$: 217.0, found 217.0

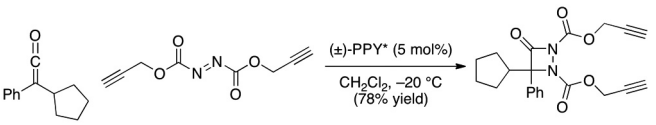

.

Dipropargyl 3-cyclopentyl-4-oxo-3-phenyl-1,2-diazetidine-1,2-dicarboxylate (ABL112) (14). In a nitrogen-atmosphere glovebox, a solution of cyclopentyl phenyl ketene (88.9 mg, 0.48 mmol, 1.0 equiv) in CH_2Cl_2 (30 mL) was prepared in a 100 mL round bottom flask. A solution of freshly prepared dipropargyl azodicarboxylate (92.7 mg, 0.48 mmol, 1.0 equiv) in CH_2Cl_2 (4 mL) was added and the flask was sealed with a rubber septum. In a glass vial, a solution of (±)-PPY* (9.0 mg, 0.024 mmol, 0.05 equiv) in CH_2Cl_2 (1 mL) was prepared and the vial was sealed with a septum cap. Both the flask and the vial were removed from the glovebox. The flask containing the golden yellow ketene/azodicarboxylate solution was cooled to −20 °C in an immersion

bath. After 20 min, the dark purple catalyst solution was added to the flask via syringe in one portion. The reaction mixture immediately darkened to a deep blue color. The mixture was stirred at −20 °C for 15 h, and then warmed to ambient temperature and concentrated under vacuum. The residue was purified by gradient flash chromatography on SiO_2 using 5–10% EtOAc in hexanes as eluent. The product was isolated as a viscous colorless oil (142.0 mg, 78% yield).

^{1}H NMR (500 MHz, $CDCl_3$) δ 7.59 (dd, $J = 7.8$, 1.4 Hz, 2H), 7.43–7.35 (m, 3H), 4.88 (app d, $J = 2.5$ Hz, 2H), 4.87–4.66 (br m, 2H), 3.02–2.93 (m, 1H), (dd, $J = 2.5$, 0.7 Hz, 1H), 2.53 (app t, $J = 2.4$ Hz, 1H), 1.90 (br s, 1H), 1.77–1.63 (m, 4H), 1.62–1.52 (m, 1H), 1.53–1.40 (m, 2H);

^{13}C NMR (125 MHz, $CDCl_3$) δ 163.9, 156.7, 147.2, 129.1, 128.7, 126.5, 76.7 (2C), 76.2, 76.1, 55.2, 54.6, 44.8, 29.0, 27.7, 25.8, 25.5;

IR (neat film, NaCl) 2950, 2871, 2361, 2330, 1836, 1773, 1741, 1449, 1436, 1377, 1307, 1267, 1224, 1187, 1128, 1062, 997 cm^{-1};

LRMS (ES+) m/z: cacld for $C_{21}H_{21}N_2O_5[M + H]^+$: 381.1, found: 381.1

1. Kidd D, Liu Y, Cravatt BF (2001) Profiling serine hydrolase activities in complex proteomes. *Biochemistry* 40:4005–4015.
2. Liu Y, Patricelli MP, Cravatt BF (1999) Activity-based protein profiling: The serine hydrolases. *Proc Natl Acad Sci USA* 96:14694–14699.
3. Patricelli MP, Giang DK, Stamp LM, Burbaum JJ (2001) Direct visualization of serine hydrolase activities in complex proteome using fluorescent active site-directed probes. *Proteomics* 1:1067–1071.
4. Martin BR, Giepmans BN, Adams SR, Tsien RY (2005) Mammalian cell-based optimization of the biarsenical-binding tetracysteine motif for improved fluorescence and affinity. *Nat Biotechnol* 23:1308–1314.
5. Blankman JL, Simon GS, Cravatt BF (2007) A comprehensive profile of brain enzymes that hydrolyze the endocannabinoid 2-arachidonoylglycerol. *Chem Biol* 14:1347–1356.
6. Jessani N, et al. (2005) A streamlined platform for high-content functional proteomics of primary human specimens. *Nat Methods* 2:691–697.
7. Washburn MP, Wolters D, Yates JR, 3rd (2001) Large-scale analysis of the yeast proteome by multidimensional protein identification technology. *Nat Biotechnol* 19:242–247.
8. Eng J, McCormack AL, Yates JR (1994) An approach to correlate MS/MS data to amino acid sequences in a protein database. *J Am Soc Mass Spectr* 5:976–989.
9. Keller A, Nesvizhskii AI, Kolker E, Aebersold R (2002) Empirical statistical model to estimate the accuracy of peptide identifications made by MS/MS and database search. *Anal Chem* 74:5383–5392.
10. Tabb DL, McDonald WH, Yates JR (2002) DTASelect and contrast: Tools for assembling and comparing protein identifications from shotgun proteomics. *J Proteome Res* 1:21–26.
11. Weerapana E, et al. (2010) Quantitative reactivity profiling predicts functional cysteines in proteomes. *Nature* 468:790–795.
12. Pearlman RS, Smith KM (1998) Novel software tools for chemical diversity. *Perspect Drug Discov* 9–11:339–353.
13. Speers AE, Cravatt BF (2004) Profiling enzyme activities in vivo using click chemistry methods. *Chem Biol* 11:535–546.
14. Berlin JM, Fu GC (2008) Enantioselective nucleophilic catalysis: The synthesis of aza-β-lactams through [2 + 2] cycloadditions of ketenes with azo compounds. *Angew Chem Int Ed Engl* 47:7048–7050.
15. Wurz RP, Lee EC, Ruble JC, Fu GC (2007) Synthesis and resolution of planar-chiral derivatives of 4-(dimethylamino)pyridine. *Adv Synth Catal* 349:2345–2352.
16. Dochnahl M, Fu GC (2009) Catalytic asymmetric cycloaddition of ketenes and nitroso compounds: enantioselective synthesis of alpha-hydroxycarboxylic acid derivatives. *Angew Chem Int Ed Engl* 48:2391–2393.
17. Allen AD BL, Gong L, Tidwell TT (1991) Cyclopropylketenes: Preparation and nucleophilic additions. *Can J Chem.* 69:138–145.
18. Mackay D, McIntryre DD, Wigle ID (1989) Anomalous shielding and hidden partner chemical exchange in the 1H NMR spectra of the bisurethane diazetidines, the 1,2-diaryl-3,5-dialkyl-6,7-dialkoxycarbonyl-4-oxo-6,7-diazabicyclo[3.2.0]hept-2-enes *J Chem Soc Perk T2* pp 1999–2010.
19. Rabjohn N (1948) Ethyl azodicarboxylate. *Org Synth* 28:58–59.

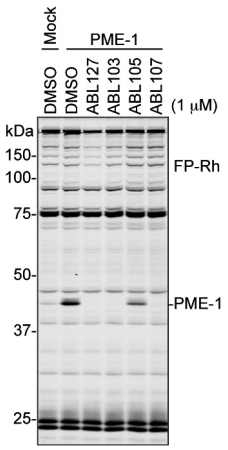

Fig. S1. Competitive ABPP in soluble lysates of PME-1-transfected HEK 293T cells (1 mg/mL protein) identifies ABLs (1 μM) as selective inhibitors of PME-1.

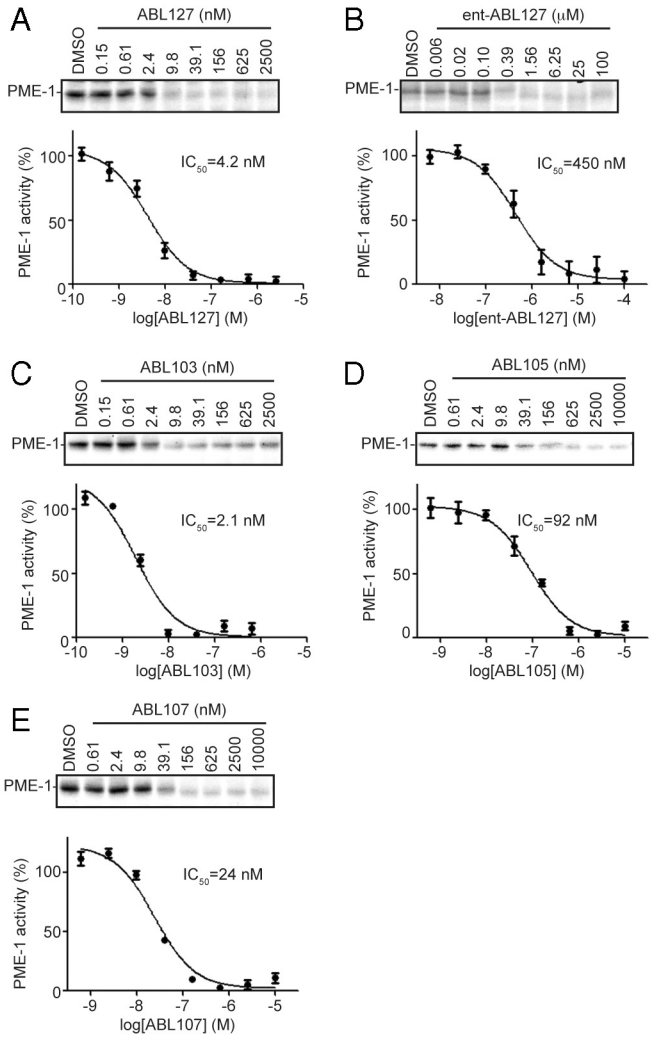

Fig. S2. Concentration-dependent PME-1 inhibition profiles in the soluble proteome of MDA-MB-231 cells (1 mg/mL protein) determined by competitive ABPP for (*A*) ABL127 ($IC_{50} = 4.2$ nM; 95% confidence limits 2.3–7.5 nM), (*B*) ent-ABL127 ($IC_{50} = 450$ nM; 95% confidence limits 240–850 nM), (*C*) ABL103 ($IC_{50} = 2.1$ nM; 95% confidence limits 0.6–7 nM), (*D*) ABL105 ($IC_{50} = 92$ nM; 95% confidence limits 50–170 nM), and (*E*) ABL107 ($IC_{50} = 24$ nM, 95% confidence limits 11–53 nM). For each profile, the region containing PME-1 of a representative competitive ABPP gel is shown above the IC_{50} curve. Data are presented as mean values ± SEM; $n = 3$/group.

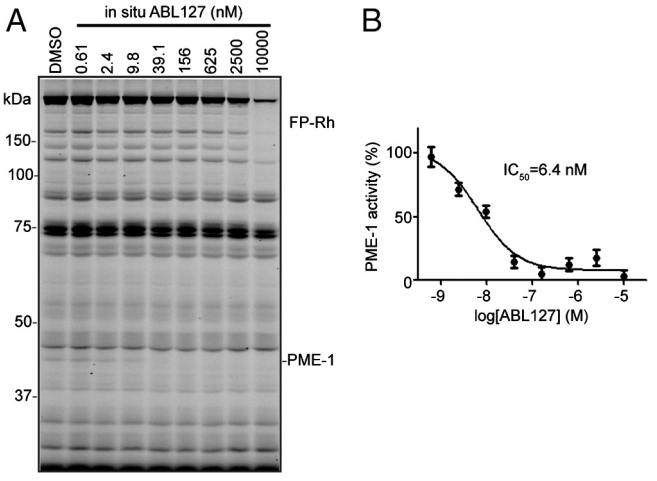

Fig. S3. ABL127 selectively inactivates PME-1 in HEK 293T cells. (*A*) Gel-based competitive ABPP profiles of the soluble proteomes from HEK 293T cells (1 mg/mL total protein) treated with a concentration range of ABL127 (0.61–10,000 nM; 1 h) reveals selective blockade of PME-1 with (*B*) an IC_{50} value of 6.4 nM (95% confidence limits 2.2–19 nM). Data are presented as mean values ± SEM; $n = 3$/group.

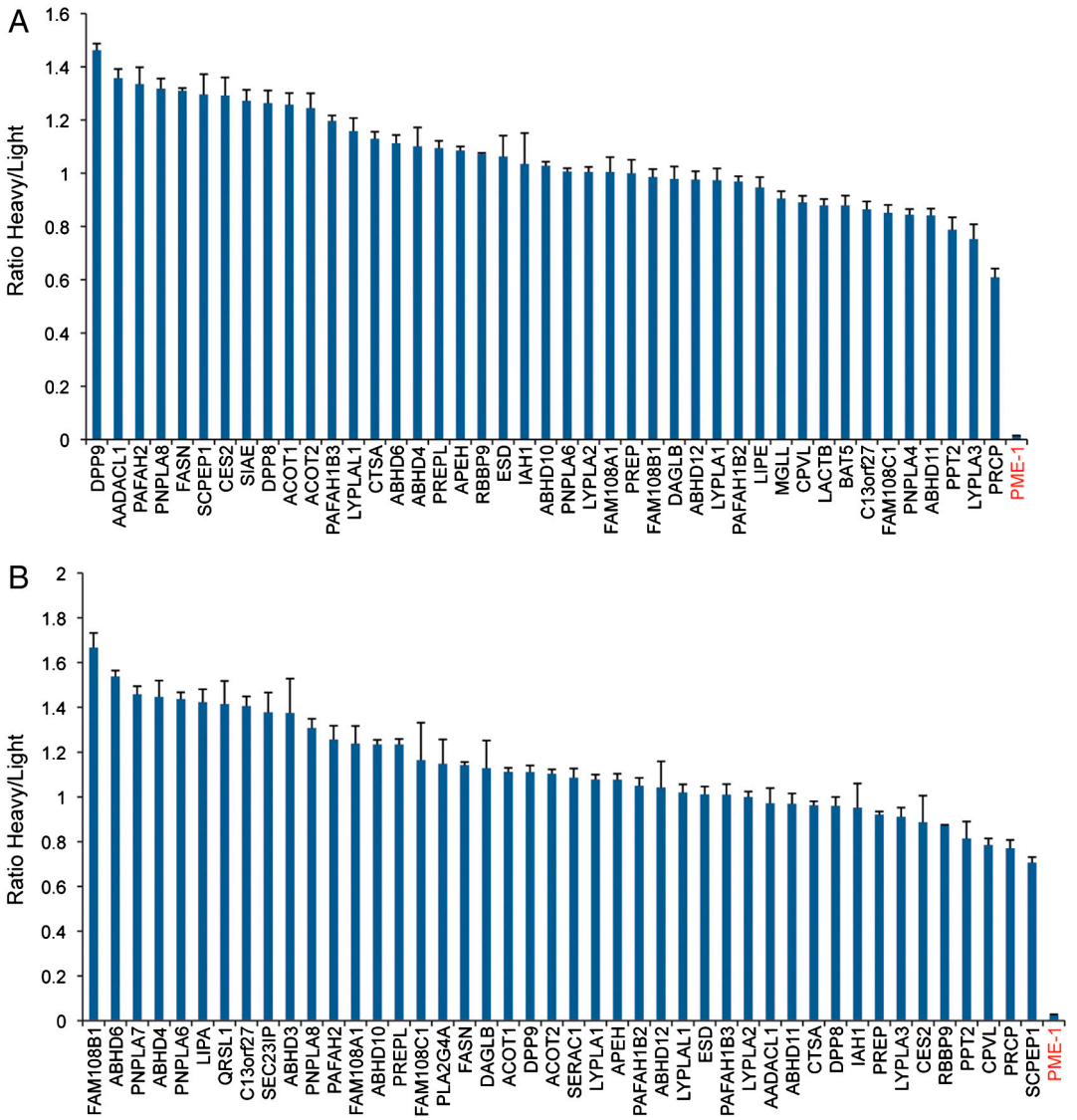

Fig. S4. SILAC-ABPP experiments reveal selective PME-1 inhibition by ABL127 in situ. (*A*) Isotopically "light" and "heavy" MDA-MB-231 cells were treated with DMSO or ABL127 (500 nM), respectively, for 1 h. Proteomes were combined in a 1:1 total protein ratio (0.5 mg each) and analyzed by ABPP-MudPIT. Serine hydrolase activities were quantified by comparing intensities of light and heavy peptide peaks. (*B*) Isotopically "light" and "heavy" HEK 293T cells were treated with DMSO and ABL127 (100 nM), respectively, for 1 h, and analyzed as described above. Data are presented as mean values ± SEM for all quantifiable peptides from each serine hydrolase.

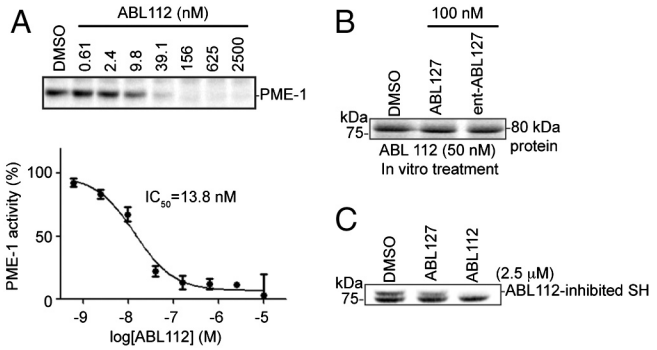

Fig. S5. Evaluation of ABL112 by competitive ABPP. (*A*) ABL112 inactivates PME-1 in the MDA-MB-231 soluble proteome (1 mg/mL protein, 1 h) with an IC_{50} value of 13.8 nM (95% confidence limits 6.5–29 nM). Data are presented as mean values ± SEM; *on* = 3/group. (*B*) MDA-MB-231 soluble lysates (0.5 mg/mL) were incubated (30 min) with DMSO, ABL127 (100 nM), or ent-ABL127 (100 nM). ABL112 (50 nM) was then added for an additional 30 minutes before performing a "click" reaction with RhN_3, followed by separation by SDS/PAGE, and visualization by in-gel fluorescence scanning. (*C*) ABL112 (2.5 μM), but not ABL127 (2.5 μM), blocks FP-Rh labeling of an approximately 80 kDa serine hydrolase in the MDA-MB-231 soluble proteome.

Table S1. Structures of all 26 ABLs in the MLPCN library

					Inactive enantiomers (of active ABLs)			
#	Structure	CID	Primary (%)	Conf (%)	#	Structure	CID	Primary (%)
1 (ABL103)	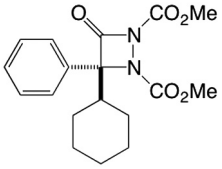	24856231	70.99	76.56q	5 (ent-ABL103)	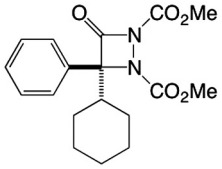	24856324	9.16
2 (ABL127)	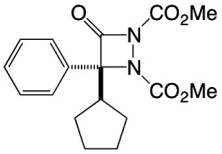	24856225	69.6	86.91	6 (ent-ABL127)	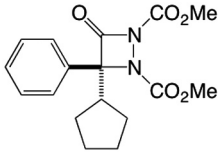	24856313	22.86
3 (ABL105)	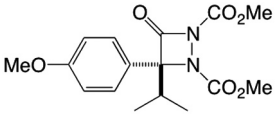	24856234	49.08	48.17	7 (ent-ABL105)	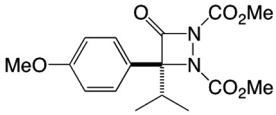	24856237	5.32
4 (ABL107)	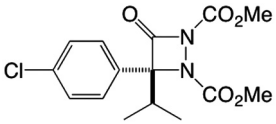	24856222	33.67	40.82				
Inactive ABLs						Inactive enantiomers (of inactive ABLs)		
8	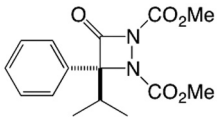	24856236	34.64	23.33	19	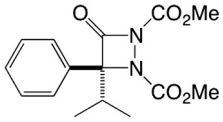	24856238	11
9	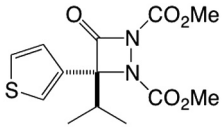	24856321	25.21	-				
10	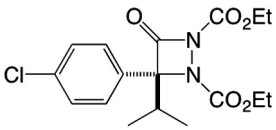	24856323	15.01	-	20	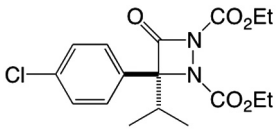	24856233	2.35
11	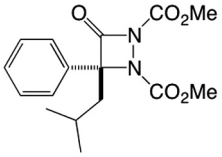	24856226	1.48	-	21	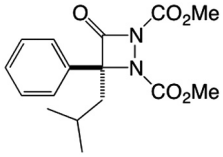	24856224	27.61
12	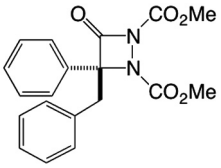	24856228	−3.25	-	22	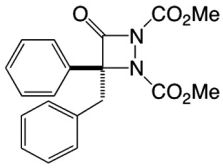	24856230	7.87

					Inactive enantiomers (of active ABLs)			
#	Structure	CID	Primary (%)	Conf (%)	#	Structure	CID	Primary (%)
13	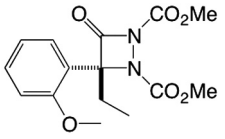	24856322	0.36	-	23	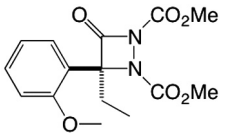	24856223	−1.97
14	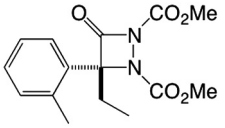	24856235	4.09	-				
15	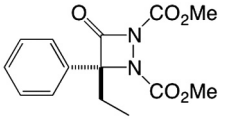	24856227	−5.78	-	24	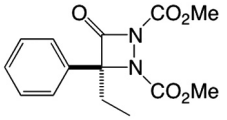	24856229	3.22
16	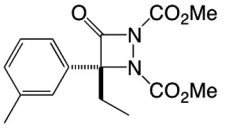	24856232	−3.06	-	25	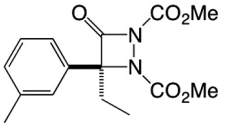	24856326	−2.44
17	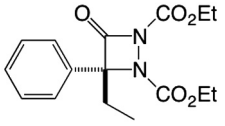	24856314	4.87	-	26	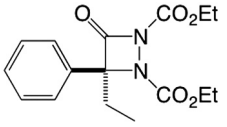	24856325	−1.35
18	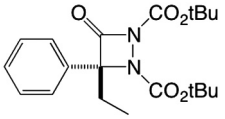	24892492	−0.67	-				

Percent PME-1 inhibition values in the primary and, if applicable, confirmation (conf) screens are shown. Complete PME-1 screening data is publicly available in the PubChem online database (http://pubchem.ncbi.nlm.nih.gov/). CID, compound identification number in the MLPCN library.